

Overload Surge Event in a Pumped-Storage Power Plant

Jiri KOUTNIK	Voith Siemens Hydro Power Generation GmbH, Germany	jiri.koutnik@vs-hydro.com
Christophe NICOLET	Ecole polytechnique fédérale de Lausanne, Switzerland	christophe.nicolet@epfl.ch
Gerald A. SCHOHL	Tennessee Valley Authority, USA	gaschohl@tva.gov
François AVELLAN	Ecole polytechnique fédérale de Lausanne, Switzerland	francois.avellan@epfl.ch

Keywords: pump-turbine, stability analysis, full-load surge, transient.

Abstract

At full load, pump-turbines operating in generating mode may experience a cylindrical cavitation vortex rope caused by the swirling flow in the draft tube cone. Under certain conditions, this vortex rope initiates both pressure and power oscillations. The hydro-acoustic analysis of a pumped storage plant experiencing such pressure and power oscillation is presented to illustrate the self induced oscillation nature of the observed event. The main physical parameters of the system stability are first introduced using a simplified 1D mathematical model of the full-load vortex rope. Then, a modal analysis of the full hydraulic circuit is performed to determine the stability domain of the plant as a function of the vortex rope parameters. Finally, a full hydro-acoustic SIMSEN model of the plant, validated with existing experimental data, is used to simulate the time sequence of the pressure surge event, and the cause of this pressure surge event is clearly identified.

Résumé

A pleine charge, les pompes-turbines fonctionnant en turbine peuvent présenter une torche de cavitation résultant de la pré-rotation de l'écoulement à la sortie de la roue. Sous certaines conditions, la torche de pleine charge génère alors des oscillations de pression et de puissance. L'analyse hydro-acoustique d'une centrale de pompage soumise à de telles oscillations de pression et de puissance est présentée pour mettre en évidence la nature auto-induite des oscillations observées lors de l'évènement. Les principaux paramètres physiques relatifs à la stabilité du système sont tout d'abord introduits à l'aide d'un modèle mathématique monodimensionnel simplifié de la torche de forte charge. Une analyse modale du circuit hydraulique dans son ensemble permet alors de déterminer les domaines de stabilité de la centrale en fonction des paramètres de la torche de cavitation. Ensuite, le modèle hydro-acoustique complet de la centrale est développé au moyen du logiciel SIMSEN. Après validation avec des mesures existantes, l'évolution temporelle des surpressions survenues au cours de l'évènement est simulée et les causes de ces surpression clairement identifiées.

Nomenclature

Term	Symbol	Definition	Term	Symbol	Definition
Cross Section Area	A	m^2	Gravity Acceleration	g	m/s^2
Absolute Mean Flow Speed	C	$C = Q/A$, m/s	Piezometric Head	h	$h = p/(\rho g) + Z$, m
Pipe diameter	D	m	Pressure	p	Pa
Machine Specific Energy	E	$E = gH_1 - gH_2$, J/kg	Hydraulic resistance	R	$R = \lambda \cdot \frac{dx}{D} \cdot \frac{ Q }{2gA^2}$ [s/m ²]
Head	H	$H = E/g$, m	Hydraulic inductance	L	$L = \frac{dx}{gA}$ [s ² /m ²]
Volume	V	m^3	Hydraulic capacitance	C	$C = \frac{gAdx}{a^2}$ [m ²]
Flow rate	Q	$Q = C \cdot A$, m ³ /s	Machine Specific Speed	v	$v = \omega \cdot \frac{(Q/\pi)^{1/2}}{(2 \cdot E)^{3/4}}$
Elevation	Z	m	Water Density	ρ	kg/m ³
Wave Speed,	a	m/s	Local Loss Coefficient	λ	-

Introduction

In higher-load operating conditions, Francis turbines can feature onset of a cavitating vortex rope in the draft tube cone which is generated by the incoming swirling flow Ref. 1. At full or overload operating conditions, the cavitation rope may under certain conditions act as an energy source, which leads to self-excited pressure oscillations in the whole hydraulic system Ref. 2. These pressure oscillations can jeopardize the mechanical and hydraulic system Ref. 3. Depending on the turbine relative location in the circuit, the turbine head may oscillate and generate power swings.

These power and pressure oscillations have been experienced at over load during commissioning tests carried out with Unit 4 of a Pumped-Storage Plant (PS Plant) located in the southeastern United States featuring four 400 MW Francis pump-turbines. The pressure surge event was well monitored and the time histories of power and wall pressure in the spiral case and draft tube cone man-doors were simultaneously recorded, see Figure 1. The event was apparently initiated by the shut down of Unit 2, with Unit 1 and Unit 3 at rest. The time sequence of the surge event onset is the following:

- Unit 4 and Unit 2 in approximately steady generating mode with Unit 1 and Unit 3 at rest;
- observation of low amplitude pressure pulsations at 2.9 Hz frequency for over load operating conditions;
- normal shut down of Unit 2;
- onset of high amplitude pressure pulsations at about 2.2 Hz frequency;

- generator power swing followed by pressure oscillations;
- standing pressure oscillations at about 2.2 Hz everywhere in the power plant piping.

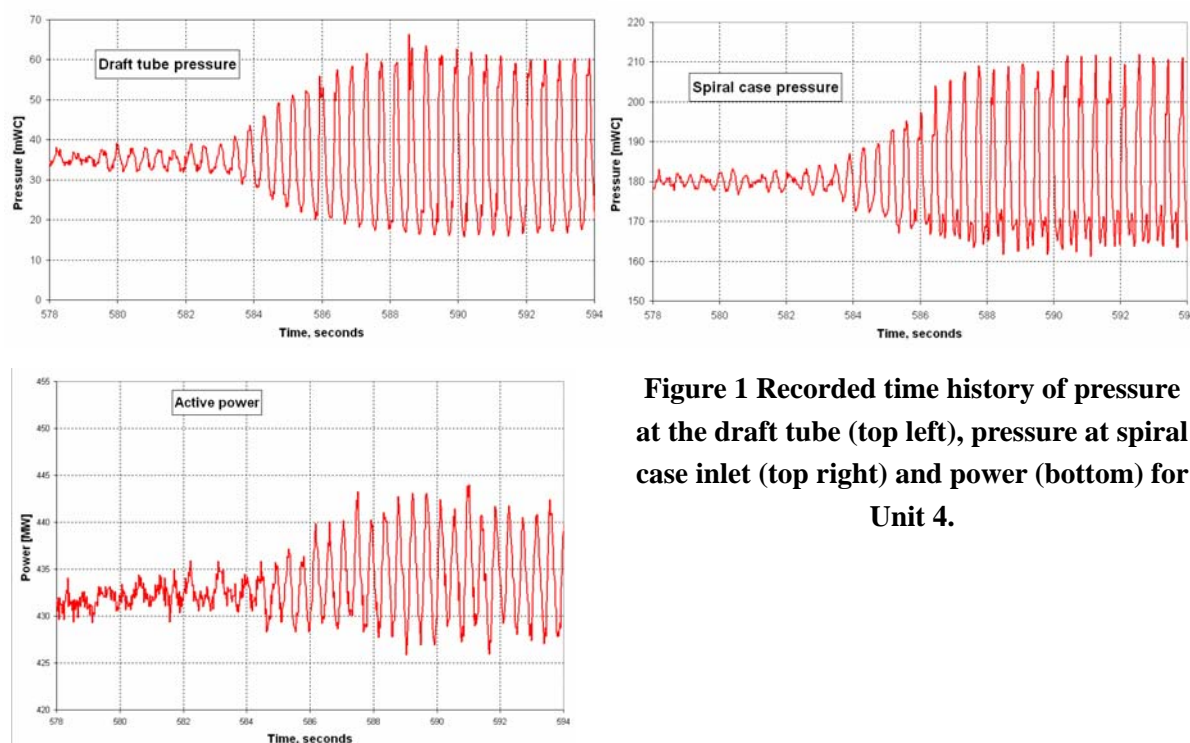


Figure 1 Recorded time history of pressure at the draft tube (top left), pressure at spiral case inlet (top right) and power (bottom) for Unit 4.

The aim of the paper is to present the hydro-acoustic analysis of the PS Plant and to show the self induced oscillation nature of the observed pressure surge event. First the main physical parameters of the system stability are introduced by using a simplified 1D mathematical model of the higher load vortex rope. Then, a modal analysis of the full hydraulic circuit is performed to determine the stability domain of the PS Plant as a function of the vortex rope parameters. Following this, a hydro-acoustic SIMSEN model of the PS Plant including the hydraulic circuit, the mechanical masses, the generators, the transformers, and the voltage regulators is developed and validated with available field experimental results of transient sequences undertaken at the PS Plant. Finally, the above described time sequence of the pressure surge event onset is simulated and analyzed, providing the cause of this pressure surge event.

Full load vortex rope – source of pressure oscillations

As the Francis turbine features blades with constant pitch, the outlet flow in the draft tube cone is optimal, almost purely axial, only for the best efficiency point. For off design operation, i.e. part load or full load, the circumferential components of the flow velocity are respectively positive or counter rotating, inducing a swirling flow Ref. 1. For full load operation and a given setting level of the machine, the swirling flow results in the development of an axi-symmetric cavitation vortex rope below the runner, see Figure 2.

For investigation of the hydro-acoustic behavior of the whole hydraulic system, we restrict

our study to a 1D approach -- more sophisticated modeling being beyond the scope of this study. The 1D approach reduces the computational time and enables parametric studies. This approach applied to the problem of modeling the cavitation vortex rope in the diffuser leads to consideration of two different components:

- a liquid conduit modeled as a "pipe" featuring inertia, compliance and friction losses;
- a gaseous volume.

The lumped component modeling of the vortex rope gaseous volume is based on the assumption that the gaseous volume V is a function of the two state variables H and Q , the net head and the discharge respectively, Ref. 4, Ref. 5 and Ref. 6. Then, the total derivative of V with respect to time at Section 2 is expressed, see Figure 3:

$$V(Q, H) \Rightarrow \left. \frac{dV}{dt} \right|_2 = \left. \frac{\partial V}{\partial H} \right|_2 \cdot \frac{dH_2}{dt} + \left. \frac{\partial V}{\partial Q} \right|_2 \cdot \frac{dQ_2}{dt} \quad (1)$$



Figure 2 Vortex rope at full load.

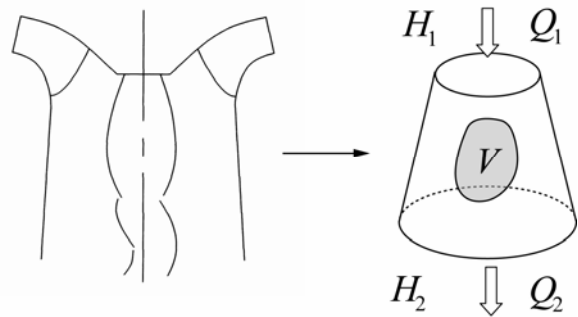


Figure 3 Indices denomination.

The rate of change of the gaseous volume is given by the variation of discharge between the 2 fluid sections limiting the rope, see Figure 3:

$$\frac{dV}{dt} = Q_2 - Q_1; \quad (2)$$

then we have:

$$Q_1 - Q_2 = C \cdot \frac{dH_2}{dt} + \chi \cdot \frac{dQ_2}{dt} \quad (3)$$

where the lumped parameters are defined as:

- the Cavity Compliance $C = -\partial V / \partial H$ [m²]; (4)

- the Mass Flow Gain Factor $\chi = -\partial V / \partial Q_2$ [s]. (5)

Moreover, we can assume that inertia and friction loss effects of the gas volume are negligible, yielding to:

$$H_2 = H_1 \quad (6)$$

First, a simple case is treated for investigating the physical parameters involved in the instability onset of a hydraulic system featuring cavitation development. The hydraulic system of interest consists of two pipes connected to the cavitation lumped element. At this stage of

study, we consider a simple symmetric case where the pipe compliance is neglected with respect to the cavitation compliance. For stability analysis purposes, it is convenient to use either a Transfer Matrix Method or an equivalent electrical system. As illustrated in Figure 4, a T shaped equivalent circuit can be setup, consisting of one resistance and one inductance modeling each pipe, on both sides of the capacitance modeling the cavitation compliance.

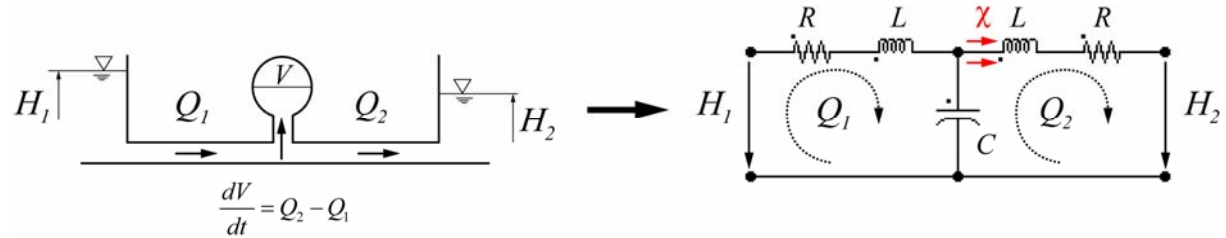


Figure 4 Stability analysis of a symmetric system with cavitation development.

The corresponding set of ordinary differential equations is the following

$$\begin{cases} H_1 = L \cdot \frac{dQ_1}{dt} + R \cdot Q_1 + H_c \\ \chi \cdot \frac{dQ_2}{dt} + C \frac{dH_c}{dt} = Q_1 - Q_2 \\ H_c = L \cdot \frac{dQ_2}{dt} + R \cdot Q_2 + H_2 \end{cases} \quad (7)$$

This system leads to the characteristic equation:

$$\left(\frac{R}{L} + X \right) \left(X^2 + \left[\frac{R}{L} + \frac{\chi}{L \cdot C} \right] \cdot X + \frac{2}{L \cdot C} \right) = 0 \quad (8)$$

yielding the following criteria for the stability of this simple system:

$$-R < \frac{\chi}{C} \quad (9)$$

The stability criteria shows that the ratio between the vortex rope mass flow gain factor and compliance, which is the vortex rope damping χ/C , must be smaller than the dissipation damping of the system to keep the system stable. The related stability domain is shown in Figure 5.

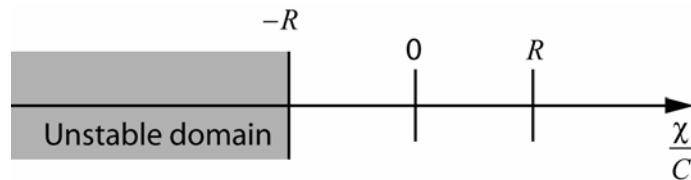


Figure 5 Stability domain regarding the vortex rope parameters.

PS Plant Modeling

The layout of the PS Plant is presented in Figure 6. A 590 meters long penstock feeds four Francis pump-turbines with four downstream surge chambers of variable cross section all connected to a 304 meters long pressurized tailrace water tunnel. The design values of the

upgraded pump-turbines are given in Table 1.

The transient behavior of the PS Plant is simulated using the EPFL software SIMSEN. This software enables simultaneous simulation of both the hydraulic and the electrical system Ref. 7. The modeling of the hydraulic components is given in Ref. 8, whereas the modeling of the synchronous generator is based on the Park's transformation described in Ref. 9. The SIMSEN model takes into account the full hydraulic system including pipes, spherical valves, downstream surge chambers, and pump-turbines. Moreover, the inertia of the rotating shaft line, the generators with saturation effects, the voltage regulators, the circuit breakers, and the transformers are included in the model. In this study, the electrical grid is considered as an infinite grid at 60Hz fixed frequency. The 1D mathematical model of the "Full-Load" vortex rope is implemented in the model. The SIMSEN layout of the PS Plant is given in Figure 7.

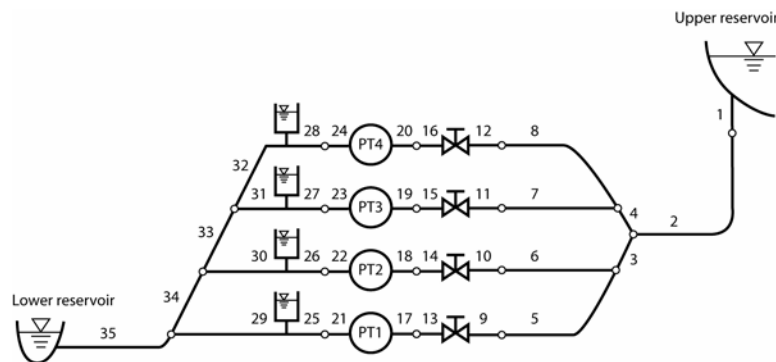


Figure 6 Layout of the Pumped-Storage Plant.

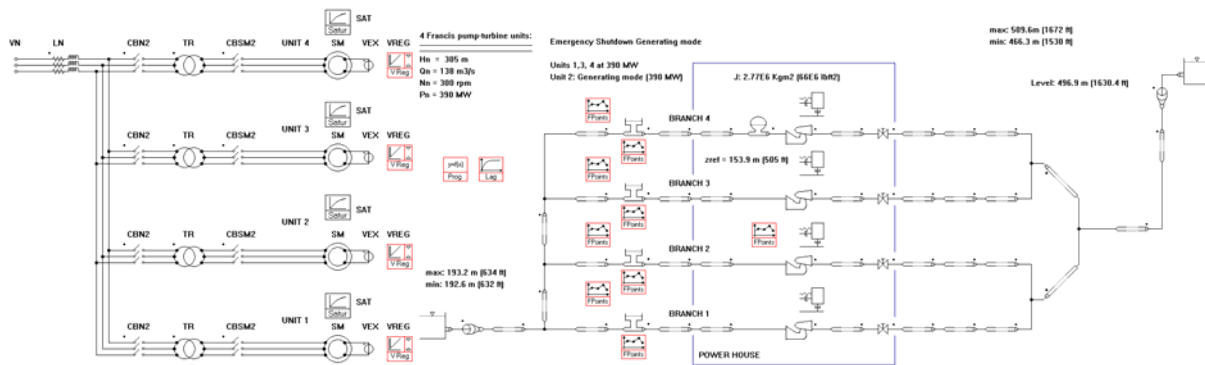


Figure 7 SIMSEN Layout of the Pumped-Storage Plant.

Table 1 : Reference values of the pump-turbine and mechanical masses inertia.

H_n [m]	Q_n [m ³ /s]	P_n [MW]	N_n [rpm]	D_{ref} [m]	$J_{rotor+turbine}$ [Kgm ²]	ν [-]
305	138	390	300	5.08	2.77e6	0.306

SIMSEN Model Validations of overall transient behavior in 1979

The validations of both the SIMSEN model and the related set of parameters are made by comparing the simulation results with available transient measurements carried out for Unit 1 during commissioning tests of the original runners in 1979. For simplicity, the simulations of emergency shutdown in both pumping and generating mode are performed without considering the electrical components and the cavitation vortex rope.

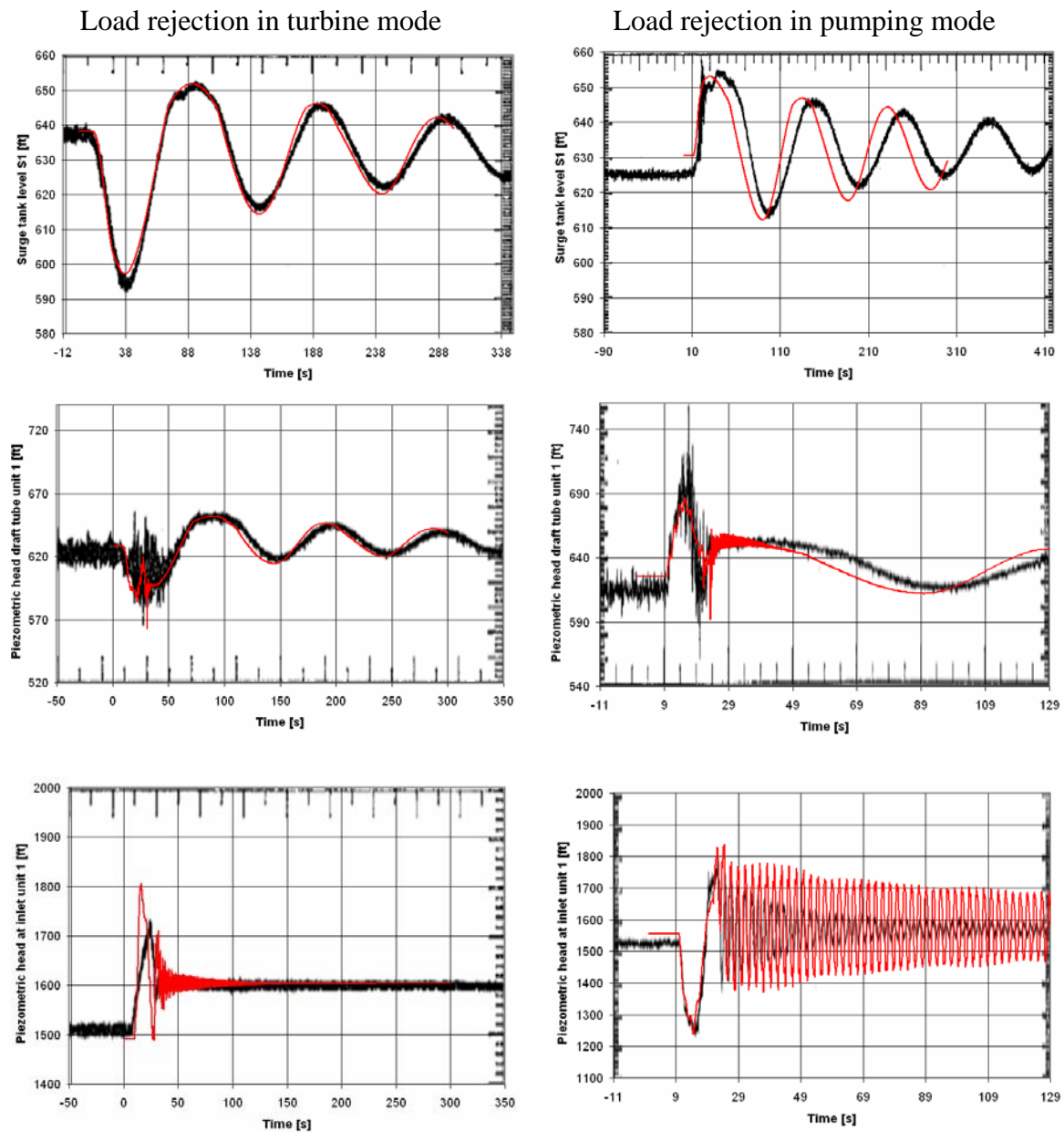


Figure 8 Comparison of SIMSEN simulation results (red line) with measurements (black line) of transients in generating and pumping modes on Unit 1 (original runner).

Case Study

The sequence of the load rejection tests in generating and pumping mode are the following:

- emergency generating shutdown test: all four units are set to fully opened guide vanes; then emergency shutdown is undertaken by simultaneously closing in 24 seconds the guide vanes following a two-slope closing law for Unit 1, Unit 3 and Unit 4; Unit 2 being kept in steady operation;
- emergency pumping shutdown test: Unit 1, Unit 3 and Unit 4 are set to 65% guide vane opening, Unit 2 being at rest; then, the three Units are shutdown simultaneously by closing the guide vanes in 16.4 seconds, following a two-slope closing law.

Simulation results

Comparisons of simulation results of the two emergency shutdowns with the measurements are made in Figure 8. For generating mode shutdown, the comparison of relevant values such as surge tank water level and draft tube piezometric head show excellent agreement while discrepancies are noticed for the spiral casing piezometric head. For the pumping mode the surge tank water level features frequency discrepancies which are due to the initial operating conditions of the units not being well fitted to the field tests. However, we focus in this paper on the stability analysis of Unit 4 in generating mode and, therefore, we may consider the parameters of the SIMSEN model properly validated for this purpose.

Event modeling - new commissioning in 2005

Modal analysis

The study of the stability of a dynamic system can be efficiently carried out using modal analysis. This analysis is performed to determine the stability domain of the hydraulic installation with respect to the lumped parameters of the vortex rope, i.e. the rope compliance and mass flow gain factor. The Transfer Matrix Method described in Ref. 10 is used with advanced models of both friction losses and damping, Ref. 11. The eigenvalues of the corresponding system global matrix are computed to derive both the natural frequencies and the damping or amplification factors of the corresponding mode from, respectively, their imaginary and real parts. The stability domain is defined as a function of both the vortex rope compliance and the mass flow gain factor in Figure 9, where the blue dots indicate unstable areas.

Given that Unit 4 experienced pressure oscillations at 2.9 Hz just prior to the event and at 2.2 Hz after the event, and assuming that the event was caused by a hydro-acoustic instability we can identify in Figure 9 the corresponding values of the vortex rope compliance and the absolute value of the mass flow gain factor. With these values for the lumped parameters of the cavitation vortex rope, we can compute, for each calculated natural frequency, both the pressure and discharge mode shapes as shown in Figure 10 for 2.2Hz. The modal analysis confirms that the maximum pressure oscillations occur close to Unit 4, which is in agreement

with the field tests, and that both the spiral casing and the draft tube experience pressure oscillations in phase, see Figure 1.

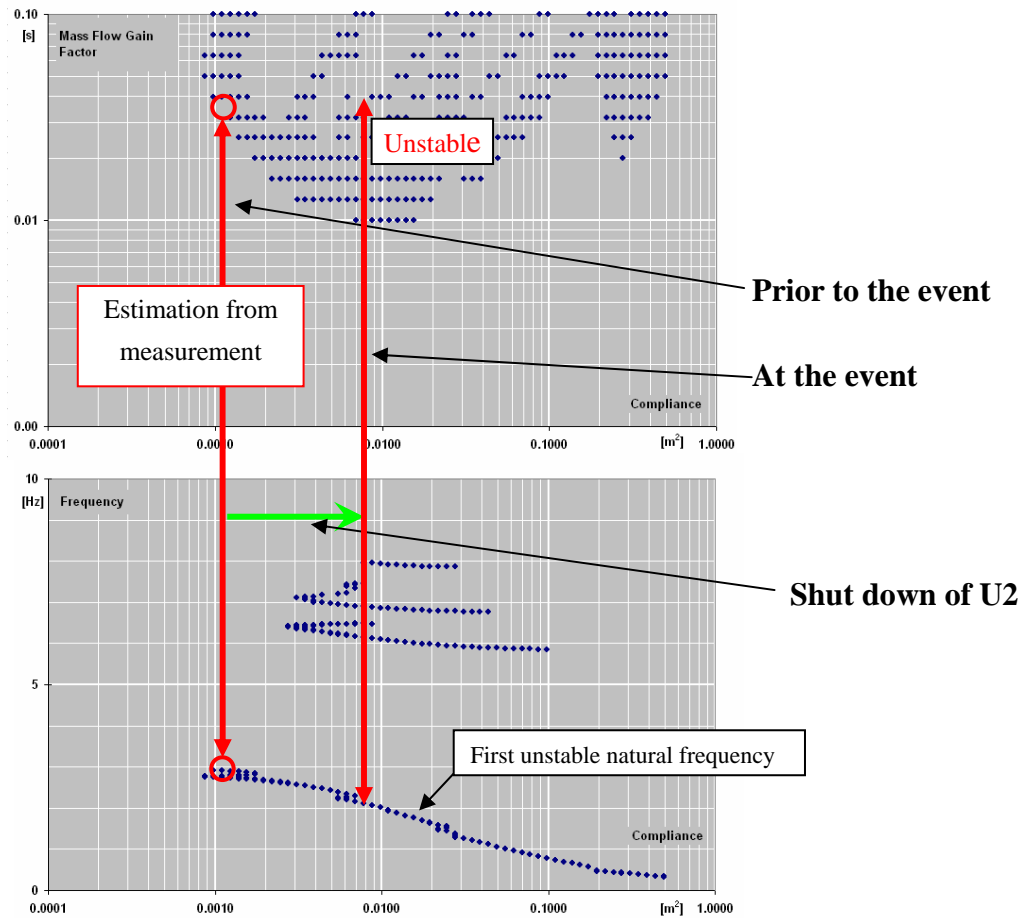


Figure 9 Stability diagram of the absolute value of the mass flow gain factor (top) and the unstable frequency (bottom) as function of Vortex rope compliance.

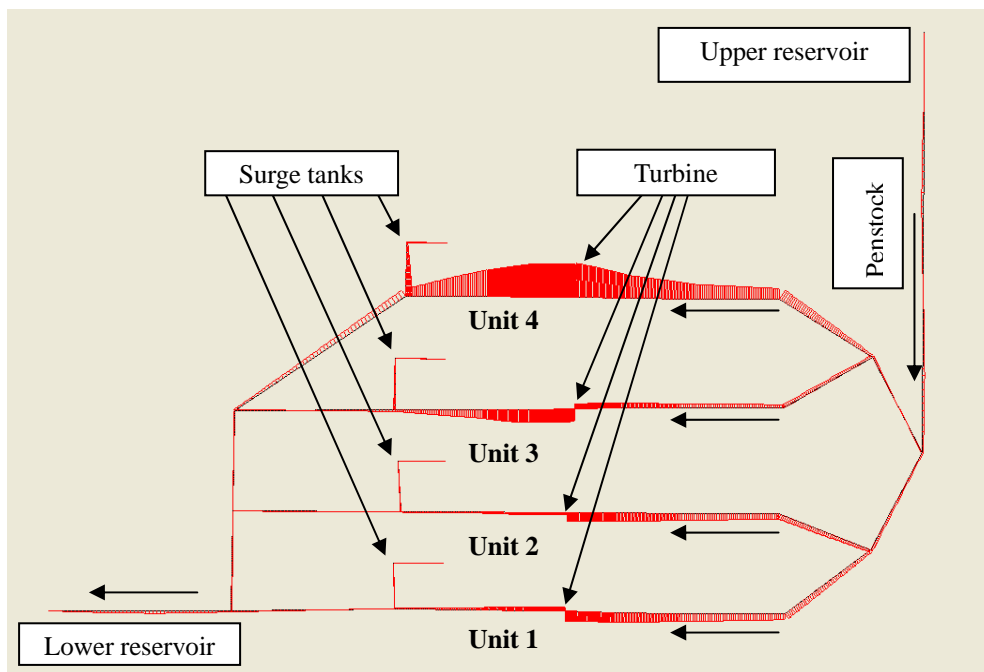


Figure 10 Pressure mode shape in the waterways, for natural frequency of 2.2 Hz.

Time domain analysis

The time domain analysis is performed with the complete SIMSEN model featuring the vortex rope model for Unit 4, the inertia of the rotating shaft line, the generators with saturation effects, the voltage regulators, the circuit breakers, and the transformers. The event is simulated according to the sequence observed on site, i.e. Unit 2 operating normally, the modernized Unit 4 in operation at overload conditions, and Unit 1 and Unit 3 at rest with guide vanes closed, and then Unit 2 is shutdown according to the normal procedure. The normal shutdown consists of closing in 24 seconds the guide vanes following a two-slope closing law and tripping the generator when 10 % of the generator power is reached.

For this analysis the vortex rope mass flow gain factor value is taken from the stability diagram, see Figure 9, for the point corresponding to the stability limit at 2.9 Hz. To take into account the influence of the operating condition on the volume of the vortex rope, the rope compliance is determined using the results of the CFD simulations for the modernized units. The draft tube flow is computed for different guide vane openings and the cavitation vortex rope volume is assumed to correspond to the volume limited by the vapor pressure iso-surface, enabling estimation of the "cavitation" volume as a function of σ , the Thoma number, and the guide vane opening, see Figure 11. A σ power law is fitted with the corresponding 80% guide vane opening overload conditions:

$$V_{rope} = A \cdot \sigma^B \quad (10)$$

where the Thoma number σ is defined as:

$$\sigma = \frac{NPSE}{E} \approx \frac{H_a - (Z_{Ref} - Z_{Tail\ Water}) - H_v}{H} \quad (11)$$

Therefore, the cavity compliance is derived according to (10):

$$C = \frac{\partial V}{\partial H_{Draft\ Tube}} \approx \frac{\partial V}{\partial Z_{Tail\ Water}} = -A \cdot B \cdot \frac{\sigma^{B-1}}{H} \quad (12)$$

The resulting estimated compliance is presented in Figure 12. However, this approach is only applicable for full load operation where pressure iso-surfaces of the flow captured by CFD computation are close to the cavity limits observed in reduced-scale model tests. For part load operation, the iso-surfaces computed by current CFD models are not close to the cavity limits observed in model tests.

The results of the time-domain analysis are presented for Unit 2 and Unit 4 in Figure 13 for the vortex rope parameters indicated as case C in Table 2, which define the system stability limit. The transient resulting from the Unit 2 shutdown induces a slow downstream pressure drop due to downstream mass oscillation. As a result, the Thoma number value of Unit 4 decreases and the vortex rope compliance increases as the vortex rope volume increases. Then, considering a constant mass flow gain factor, the vortex rope compliance increases until the unstable domain of operation is reached; leading to the pressure oscillation onset in

the draft tube; the system being in self-excited conditions. Then the system remains unstable as long as the sigma value (i.e.the vortex rope size) does not reach the same steady value as prior to the event. The calculated oscillation frequency corresponds well with the measured frequency value, whereas the agreement between the calculated and measured amplitudes is less good.

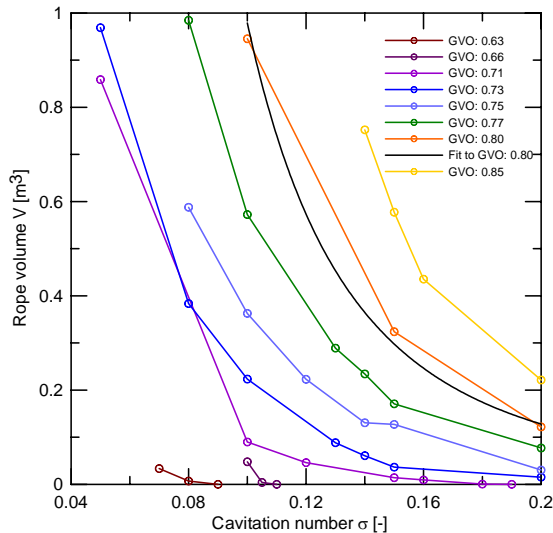


Figure 11 Vortex rope volume at full load computed with CFD.

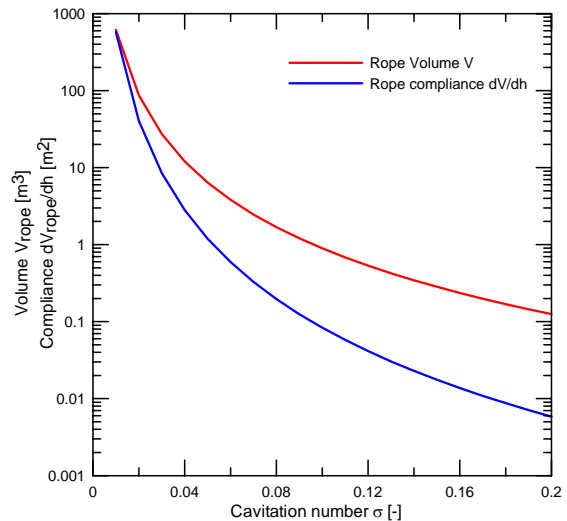


Figure 12 Vortex rope compliance.

A parametric study of the influence of the vortex rope is carried out using the values given in Table 2. For case A, the mass flow gain factor and compliance are both kept constant. For cases B, C and D, the cavity compliance is taken as a function of the Thoma number and the head, and the mass flow gain factor is still kept constant. The resulting draft tube piezometric heads are presented in Figure 14. In case A, the amplitudes increase dramatically. Case B exhibits amplitudes that are strongly affected by the compliance dependence on the Thoma number value. Case C corresponds to the limit of stability with bounded amplitudes. In case D, the self-excitation is initiated but the oscillations are damped once the surge chamber level recovers its initial value. This sensitivity analysis shows clearly that the shutdown of Unit 2 initiates the self-excitation mode by decreasing the Unit 4 draft tube pressure and, consequently, the Thoma number value.

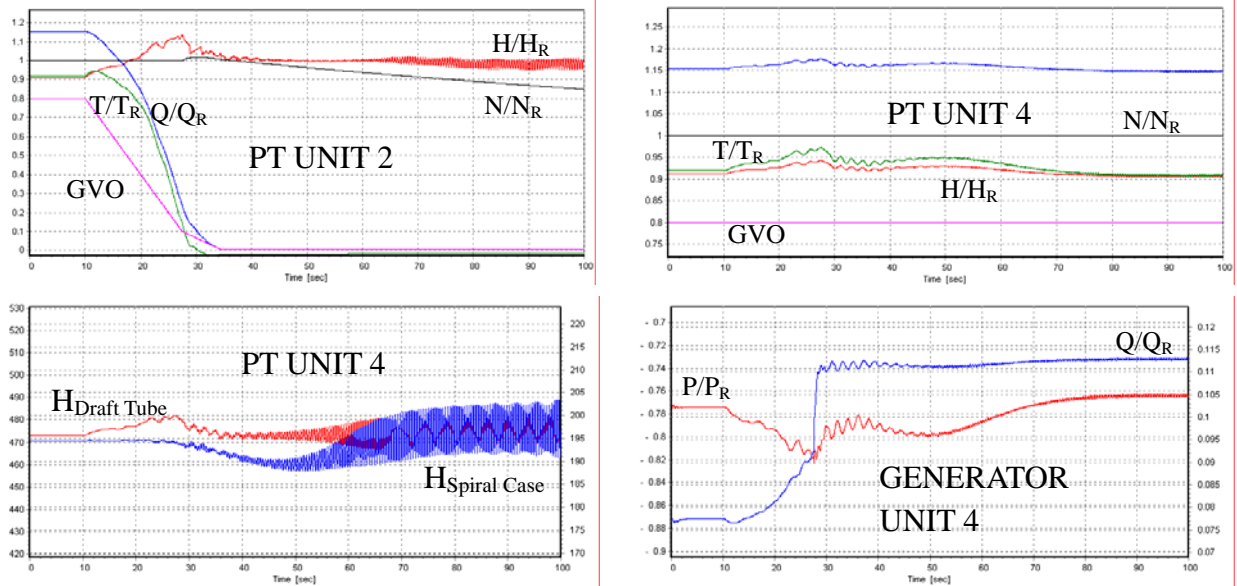


Figure 13 Simulation results of the transient of the pump-turbine of Unit 2 and Unit 4.

Table 2: Vortex rope parameters for 4 simulation cases.

Cases	A	B	C	D
Compliance C [m ²]	10^{-2}	$C = C(\sigma, H)$	$C = C(\sigma, H)$	$C = C(\sigma, H)$
Mass flow gain factor χ [s]	-0.005	-0.005	-0.004	-0.003

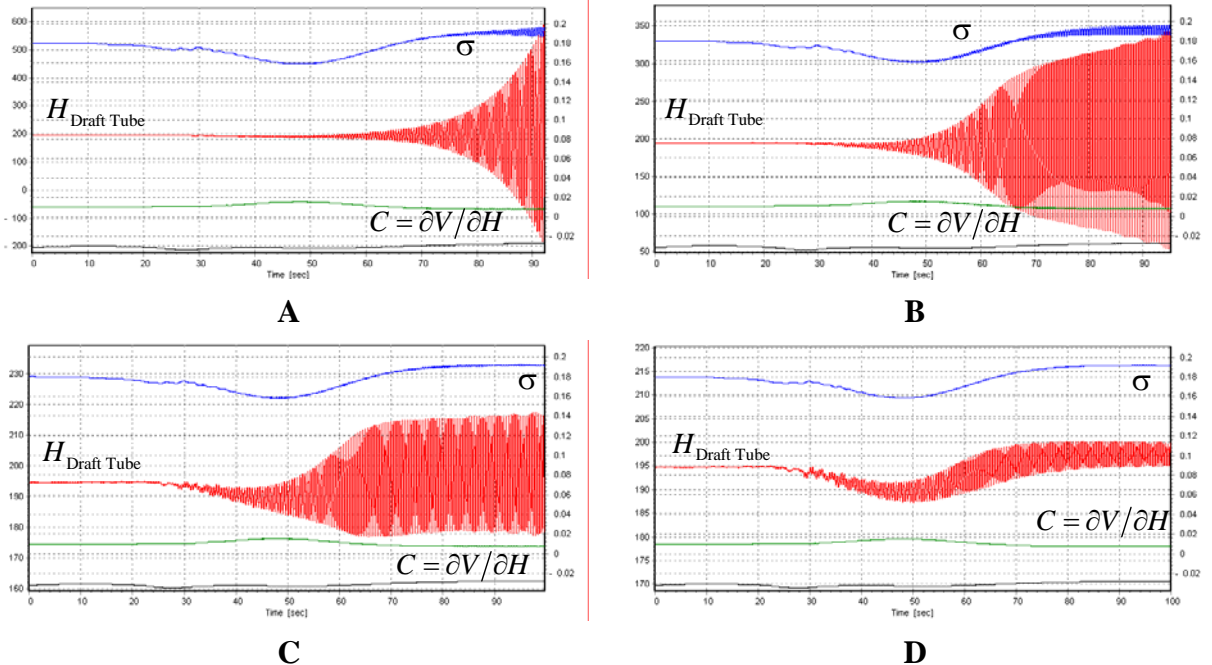


Figure 14 Simulation results of the draft tube pressure oscillations of Unit 4 for the rope parameters of Table 2.

Summary and conclusions

An overload surge phenomenon was experienced at a pumped storage plant during over operating range tests. In order to have a better understanding of the onset condition of this phenomenon, a one-dimensional model of the power plant, including a model of the vortex rope, is carried out. The vortex rope at higher load conditions is modeled by defining a compliance parameter and a mass flow gain factor for the cavitation volume. Using this simplified model, the stability domain of the power plant with respect to the vortex rope parameters is determined through modal analysis and the vortex rope parameters for the power plant are estimated by locating the observed test conditions within the stability domain. Then, a time domain simulation of the dynamic behavior of the power plant according to the event time sequence observed on site is performed. The simulation model includes the hydraulic system with a non-linear vortex rope model, the rotating inertias, the electrical components, and the governors. In an original approach, the vortex rope cavitation compliance is modeled as a non-linear function of the Thoma number and the head, where the function is determined by comparison of results from scale-model experiments and CFD modeling. The simulation results show the role played in this case by the shutdown of a neighboring unit, which decreases the pressure downstream of the affected unit and, therefore, the cavitation number and eventually initiating the self-excited surge.

The comparison of calculated and measured results shows surprisingly good agreement considering the relatively simple model used for the complex flow - vortex rope structure within the pump-turbine. Moreover, this investigation provides a deeper insight into the physical phenomena underlying the onset of overload pressure surge. However, to be predictive, the hydro-acoustic modeling requires a very accurate set of data provided from either reduced scale model measurements or advanced unsteady two-phase flow analysis.

Acknowledgement

The authors would like to thank Mr. Gary Franke from VSH York, USA, for the CFD computations. For this paper, the authors took advantages of the development of the SIMSEN hydraulic extension, developed in collaboration with Mr. Philippe Allenbach, Dr. Alain Sapin, and Prof. Jean-Jacques Simond from the EPFL Laboratory for Electrical Machines under the following contract awards: CTI No 5750.1 EBS, PSEL No 215 Scapin, EDF-CIH, HMD 420.210.3459.

References

- Ref. 1 Nishi, M., "Surging characteristics of conical and elbow type draft tubes." Proceeding of the 12th IAHR Symposium, Stirling, p272-283, 1984.
- Ref. 2 Jacob, T., "Evaluation sur modèle réduit et prediction de la stabilité de fonctionnement des turbines Francis", Thesis, EPFL-N° 1146, Lausanne, 1993.
- Ref. 3 Jacob, T., Prénat, J.-E., Vullioud, G., Lopez Araguas, B., "Surging of 140 MW Francis turbines at high load, analysis and solution", Proc. 16th Symp. IAHR, Sao Paolo, 1992.

- Ref. 4 Brennen, C., Acosta, A. J., “Theoretical, quasi-static analysis of cavitation compliance in turbopumps”, *J. Spacecraft*, Vol. 10, NO. 3, March 1973, pp. 175-180.
- Ref. 5 Brennen, C., Braisted, D.M. “Stability of hydraulic systems with focus on cavitating pumps”, *IAHR Symposium*, 1980, Tokyo, Session V, 11p.
- Ref. 6 Koutnik, J., Pulpitel, L. “Modeling of the Francis turbine full-load surge”, *Modeling, Testing and Monitoring for Hydro Power plants – II*, Lausanne, July 1996, Session III, p.143-154.
- Ref. 7 Nicolet, C., Avellan, F., Allenbach, P., Sapin, A., Simond, J.-J., Hérou, J.-J. “Transient phenomena in Francis turbine power plants: Interaction with the power network”, *IAHR WG1*, 2003, Stuttgart.
- Ref. 8 Nicolet, C., Avellan, F., Allenbach, P., Sapin, A., Simond, J.-J., Kvicinsky, S., Crahan, M. "Simulation of Transient Phenomena in Francis Turbine Power Plants : Hydroelectric Interaction ". *Proceedings of Waterpower XIII, Advancing Technology for Sustainable Energy*, Buffalo, N.Y., USA, July 2003.
- Ref. 9 Canay I. M. “Extended synchronous machine model for calculation of transient processes and stability”. *Electric machines and Electromechanics*, 1977, Vol.1, 137-150.
- Ref. 10 Streeter, V. L., Wylie, E.B. “Hydraulic transients”, *Mc Graw-Hill*, 1967.
- Ref. 11 Haban, V., Koutnik, J., Pochyly, F., ”1-D mathematical model of high-frequency pressure oscillations induced by RSI including an influence of fluid second viscosity”, *Proceedings XXIst, IAHR 2002*, Lausanne, pp. 735-740.